The International Journal of Advanced Manufacturing Technology (2019) 105:3233–3247
https://doi.org/10.1007/s00170-019-04431-5

ORIGINAL ARTICLE

Experimental investigation of the application of parameter inversion for residual stress adjustment in five-axis milling using an annular cutter

Kun Huang[1] · Wenyu Yang[2] · Yi Gao[2] · Xiaoming Ye[3]

Received: 23 March 2019 / Accepted: 17 September 2019 / Published online: 11 November 2019

Abstract
Five-axis milling makes it possible to control the relative pose between a tool and surface normal of a workpiece, and is widely used in manufacturing. In this study, an experimental investigation of the application of parameter inversion for residual stress adjustment in five-axis milling has been conducted based on two methods: an orthogonal experiment with interaction of factors and a random setting of the expected residual stress. The results of the orthogonal experiment with interactions of factors show that the significance of the influence of the machining parameters on the residual stress obtained with parameter inversion is similar to the experimental results. The results of the experiment with a random setting of the expected residual stress show that the average of the difference between the measured and expected results for the 30 cutting conditions is only 0.3951 MPa, which indicates that residual stress prediction using parameter inversion is statistically effective. Moreover, the results show that using parameter inversion, the correctness of the prediction of compressive and tensile residual stress is 73.33%, which is higher than the 50% value that is achievable without any adjustment. Overall, the results of the experimental investigation in this paper show that residual stress adjustment based on parameter inversion is applicable for five-axis milling, which shows the potential of this adjustment method for industrial applications.

Keywords Machining · Orthogonal experiment with interaction of factors · Residual stress · Parameter inversion

1 Introduction

Five-axis milling makes it possible to accurately control the relative pose between a tool and the surface normal of a workpiece, which is very useful for improving the cutting conditions of the tool insert and enhancing machining efficiency and geometric accuracy. It has been widely used for manufacturing parts with complex surfaces, such as die surfaces and integral impellers. It is worth noting that when machining these complex surfaces using five-axis milling, the angle between the tool and the surface normal of the workpiece cannot be set arbitrarily, as it is constrained by the overall shape of the workpiece to avoid interference between the tool and workpiece. However, when machining surfaces with a large radius of curvature, such as turbine blades and controllable-pitch propellers, the angle between the tool and surface normal of the workpiece can be set in a wide range. In these cases, a cutting tool with an annular cutter can be used. Compared to ball end milling, machining with an annular cutter is more efficient, particularly for machining large parts. However, these types of parts (e.g., turbine blades and controllable-pitch propellers) bear alternating loads in service, which means that residual stress in the machined surface layer of the parts will impact their service life [1]. Because machining is usually used as the final

✉ Kun Huang
khuang123456@163.com

✉ Wenyu Yang
mewyang@hust.edu.cn

[1] Guangdong Bright Dream Robotics CO. LTD., Guangdong Province, Foshan 528311, China

[2] State Key Laboratory of Digital Manufacturing Equipment and Technology, School of Mechanical Science and Engineering, Huazhong University of Science and Technology, Wuhan 430074, China

[3] School of Energy and Power Engineering, Huazhong University of Science and Technology, Wuhan 430074, China

procedure to guarantee the geometric accuracy of parts, residual stress induced by milling will directly affect the service life of the parts. Therefore, research on residual stress adjustment for five-axis milling using an annular cutter is important.

Machining-induced residual stress is affected by both mechanical stress and thermal stress [2]. The distribution of mechanical and thermal stress is influenced not only by the amplitude of the cutting force and the cutting temperature but also by their distribution area [3, 4]. In general, the cutting force amplitude, cutting temperature, and their distribution area are determined by the geometry of the uncut chip. For example, in external turning, the geometry of the uncut chip is generally determined by the feed rate and depth of cut. The cutting speed can affect the shear angle, which will also affect the geometry of the uncut chip. Huang et al. [5] experimentally investigated the effects of the cutting speed, feed rate, and depth of cut on the temperature penetration depth using a physical vapor deposition method. The results indicated that even though the cutting force increases with increasing feed rate, the maximum cutting temperature decreases. This is because the distribution areas for the cutting force and cutting heat increase with increasing feed rate, which results in a reduction in the maximum cutting temperature. For theoretical modeling, Komanduri and Hou [6] constructed an analytical model of the cutting temperature field for orthogonal cutting by introducing mirror heat source. Based on their work, Huang and Yang [7] improved the model by introducing the heating time, which is affected by the contact length of the heat source. However, the contact length of the heat source is affected by the uncut chip thickness and shear angle, demonstrating the importance of the uncut chip geometry for the cutting temperature field. Based on the above temperature field model, Huang et al. [8] constructed an analytical model of the stress field during orthogonal cutting. The computed stress field is more consistent with photoelasticity experimental results than traditional models. This stress field model could provide more accurate stress inputs for residual stress models. Huang and Yang [9] then improved the analytical model for the residual stress based on the above stress field model by introducing initial conditions, making it possible to obtain a unique solution for the residual stress during stress relaxation procedures. This improved residual stress model established mapping relationships between the input parameters and residual stress, which can be used to analyze the mechanism by which the input parameters influence the residual stress. With the introduction of a multivariable decoupling method, Huang and Yang [10] investigated the influence of parameters including the shear angle, depth of cut, and rake angle on the residual stress. The results show that in theory, when the tool geometry and workpiece material are unchanged, the residual stress is determined by the cutting speed and the geometry of the uncut chip.

For milling processes, even though the geometry of the uncut chip is more complex than in orthogonal cutting, it can be determined by five machining parameters: the feed rate, front obliquity, side dip angle, depth of cut, and residual height (note that the residual height represents the cutting row spacing in milling processes). Similarly, when the tool geometry and workpiece material are unchanged, the residual stress induced by milling can be determined by the cutting speed and the geometry of the uncut chip. Therefore, there are a total of six machining parameters that determine the machining-induced residual stress, which is very similar to the six spatial degrees of freedom necessary to determine the endpoint of a gesture for a robot; the cutting speed, front obliquity, and side dip angle correspond to rotational degrees of freedom, while the feed rate, depth of cut, and residual height correspond to translational degrees of freedom. Note that because three-axis or four-axis milling cannot be used to control the angle between a tool and the surface normal of a workpiece when milling a curved surface, they cannot be used to control the geometry of the uncut chip. Therefore, in theory, they cannot be used to control the residual stress during milling of a curved surface.

The importance of residual stress for the service life of parts has been emphasized by numerous studies. Chen et al. [11] investigated the role of residual stress in stress corrosion cracking at neutral pH. The results indicate that the tensile residual stress is a large mechanical driving force for crack nucleation and short crack growth. Withers [12] reviewed the effect of residual stress on fatigue. The results showed a series of the effects of residual stress on plastic collapse, fracture, fatigue, thermal fatigue, creep cavitation cracking, and stress corrosion. To obtain parts with a longer service life for industrial requirements, it is important to be able to predict the expected residual stress. Then, in order to obtain the desired residual stress, it is necessary to determine the input parameters that correspond to the desired residual stress. However, for machining-induced residual stress, the existing studies have typically focused on constructing the mapping relationships from the machining parameters, tool parameters, and workpiece material to the residual stress. For example, Arrazola et al. [13] presented recent advances in modeling metal machining processes. These studies have tended to establish a model to predict the residual stress with known input parameters. Brinksmeier et al. [14, 15] proposed a concept called Process Signatures, which aims to solve the inverse surface integrity problem in machining process, i.e., to find appropriate cutting parameters based on surface integrity. Because in actual machining processes, it is necessary to determine the input machining parameters that correspond to an expected residual stress. Huang et al. [16] addressed this problem by proposing a method to control machining-induced residual stress using parameter inversion, which could be used to compute the input machining parameters (e.g., the cutting

Table 1 Tested values for each machining parameter

	1 Feed rate (mm/tooth)	2 Cutting speed (mm/s)	3 Front obliquity (°)	4 Side dip angle (°)	5 Residual height (mm)	6 Depth of cut (mm)
1	0.02	400	6	0	0.005	0.5
2	0.06	800	10	*3*	0.01	1
3	*0.09*	*1300*	*14*	6	*0.02*	*1.5*
4	0.12	1900	18	9	0.04	2
5	0.14	2500	22	12	0.07	2.5

speed and feed rate) based on the desired residual stress. Using the computed input machining parameters, the expected residual stress can be achieved. However, the method in that study is focused on orthogonal cutting and an analytical model for the residual stress, and requires further research for the purpose of industrial application. In this study, residual stress adjustment based on parameter inversion for five-axis milling using an annular cutter is studied and verified.

1.1 Nomenclature

OIndex of output (residual stress)
A_iInput parameter
a_{i0}Reference value for A_i
$H(a_{10}, a_{20}, \ldots, a_{i0}, \ldots, a_{n0})$Reference value of O computed using $a_{10}, a_{20}, \ldots, a_{i0}, \ldots, a_{n0}$
$O(A_i)$Fitting function for O with A_i
ΔO^{A_i} Change in O caused by a change in A_i

2 Establishment of parameter inversion for five-axis milling-induced residual stress adjustment

2.1 Fitting curves for the input parameters and residual stress

According to the theory of parameter inversion for residual stress adjustment proposed in a previous paper of Huang et al. [16] (as mentioned in Section 1), reference values for the input parameters and fitting curves for the input parameters with the residual stress should be determined. For the five-axis milling in this study, there are six input machining parameters: the feed rate, cutting speed, front obliquity, side dip angle, residual height, and depth of cut. When the cutting tool and workpiece material are unchanged, the residual stress can be determined using these six machining parameters. To construct fitting curves for these machining parameters with the residual stress, each parameter was assigned 5 values, as listed in Table 1, in which the reference values for the machining

Table 2 Cutting conditions and corresponding residual stresses (the cutting condition for the reference machining parameters and resulting residual stress is in italics)

No.	1 Feed rate (mm/tooth)	2 Cutting speed (mm/s)	3 Front obliquity (°)	4 Side dip angle (°)	5 Residual height (mm)	6 Depth of cut (mm)	Average measured residual stress (MPa)
1	**0.14**	1300	14	3	0.02	1.5	− 9.23
2	**0.12**	1300	14	3	0.02	1.5	− 14.91
3	***0.09***	*1300*	*14*	*3*	*0.02*	*1.5*	*− 4.58*
4	**0.06**	1300	14	3	0.02	1.5	− 17.69
5	**0.02**	1300	14	3	0.02	1.5	19.74
6	0.09	**2500**	14	3	0.02	1.5	− 1.66
7	0.09	**1900**	14	3	0.02	1.5	10.27
8	*0.09*	***1300***	*14*	*3*	*0.02*	*1.5*	*5.24*
9	0.09	**800**	14	3	0.02	1.5	5.49
10	0.09	**400**	14	3	0.02	1.5	− 13.51
11	0.09	1300	**22**	3	0.02	1.5	− 27.01
12	0.09	1300	**18**	3	0.02	1.5	− 16.66
13	*0.09*	*1300*	***14***	*3*	*0.02*	*1.5*	*3.89*
14	0.09	1300	**10**	3	0.02	1.5	6.68
15	0.09	1300	**6**	3	0.02	1.5	7.69
16	0.09	1300	14	**12**	0.02	1.5	2.80
17	0.09	1300	14	**9**	0.02	1.5	10.46
18	0.09	1300	14	**6**	0.02	1.5	8.37
19	*0.09*	*1300*	*14*	***3***	*0.02*	*1.5*	*2.46*
20	0.09	1300	14	**0**	0.02	1.5	− 2.95
21	0.09	1300	14	3	**0.07**	1.5	19.61
22	0.09	1300	14	3	**0.04**	1.5	14.58
23	*0.09*	*1300*	*14*	*3*	***0.02***	*1.5*	*29.61*
24	0.09	1300	14	3	**0.01**	1.5	− 7.15
25	0.09	1300	14	3	**0.005**	1.5	23.33
26	0.09	1300	14	3	0.02	**2.5**	29.79
27	0.09	1300	14	3	0.02	**2**	13.43
28	*0.09*	*1300*	*14*	*3*	*0.02*	***1.5***	*7.92*
29	0.09	1300	14	3	0.02	**1**	− 5.39
30	0.09	1300	14	3	0.02	**0.5**	36.12

Average residual stress for the reference machining parameters (after removal of the maximum and minimum values): $H(a_{10}, a_{20}, a_{30}, a_{40}, a_{50}, a_{60})$ = (5.24 + 3.89 + 2.46 + 7.92)/4 = 4.88 MPa

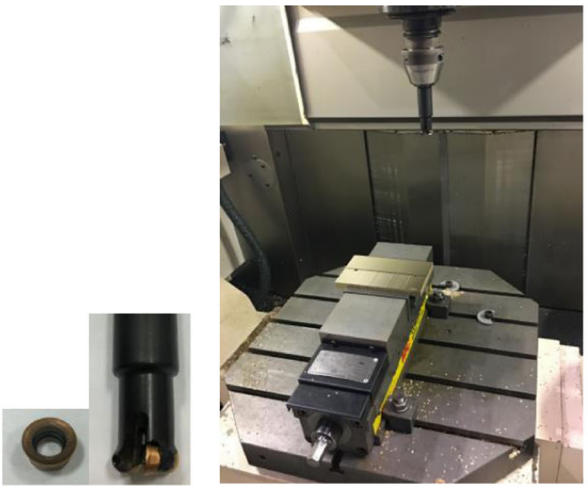

(a) Cutting tool (b) Machine tool

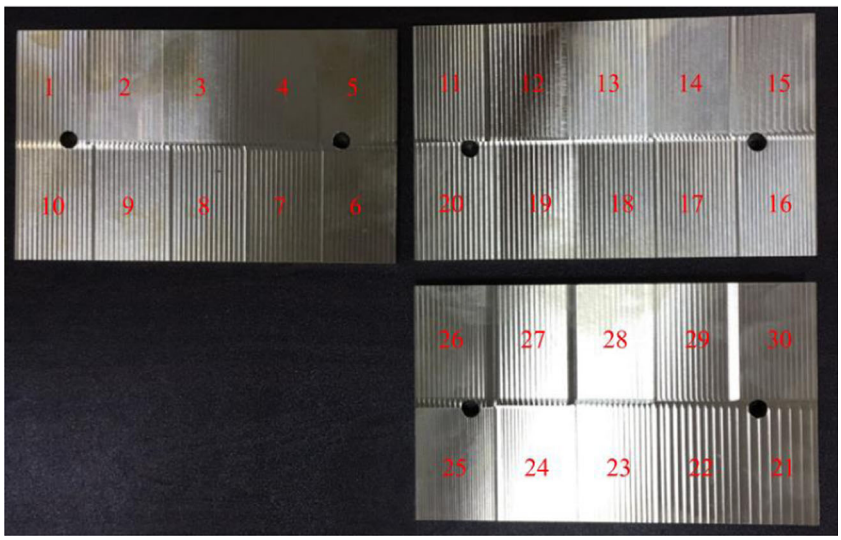

(c) Workpiece

Fig. 1 **a** Cutting tool (Sandvik annular cutter, No. 600-1045E-ML1030), **b** machine tool (Kikron UCP 800 Duro), and **c** workpiece (nickel aluminum bronze alloy) used in this study

parameters are given in italic. Note that in this paper, reference values were selected based on the requirement of semi-finishing in five-axis milling. It depends on the requirement of the users. A series of cutting conditions can then be designed, as summarized in Table 2. Note that the reference machining parameters are repeated 6 times: in rows 3, 8, 13, 19, 23, and 28.

For the milling processes using the cutting conditions in Table 2, a Sandvik annular cutter (No. 600-1045E-ML1030) was used to machine a nickel aluminum bronze alloy with a Kikron UCP 800 Duro machine tool, as shown in Fig. 1. Three workpieces were used. To reduce positioning error for each clamping, the cutting area was successive for each five cutting conditions listed in Table 2. The residual stress measurements were based on the energy-based method improved by Jin et al. [17]. In that study, an improved energy-based method was proposed to measure the equi-biaxial residual stress of bulk materials using spherical indentation. More details on this method can be found in [17]. The residual stresses were all measured using the same equipment, as shown in Fig. 2. Therefore, systematic errors are the same for all of the measurement data in this study. Moreover, for each cutting condition, the residual stress was measured at nine sample points (the total number of sample points for all cutting conditions is thus $9 \times 30 = 270$), and the average values are used to represent the residual stress corresponding to each cutting condition (original measurement data is provided in Table 8 of the Appendix). This allowed a higher reliability of the mapping relationship

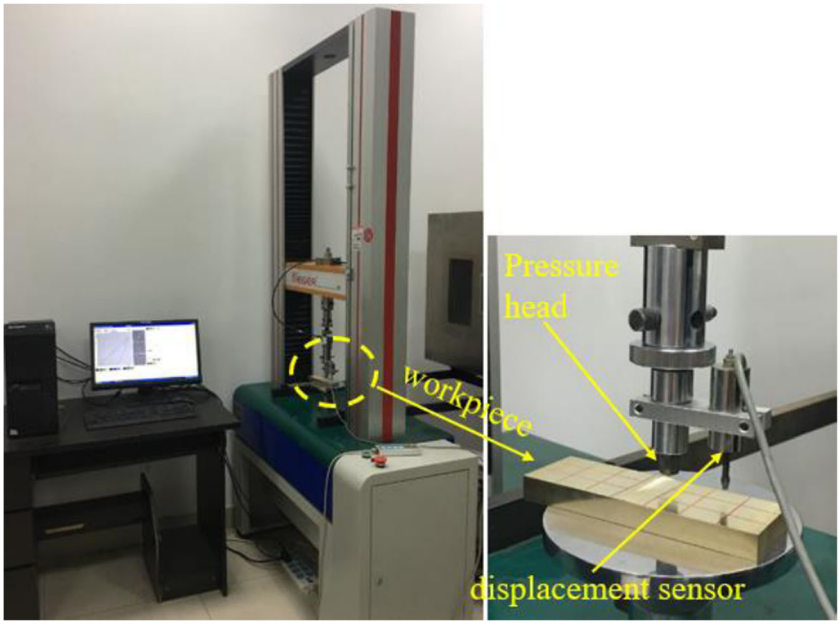

Fig. 2 Setup for the measurement of residual stress based on the energy-based method

between the measured residual stress and machining parameters to be obtained. The average residual stress for each cutting condition is listed in the rightmost column of Table 2.

As shown in Table 8 of the Appendix, the difference among the data from the nine sample points is large. The first reason is that the sample points in the same case are selected in different positions in the area machined using the same cutting parameter. The data of the sample points was not repeatedly measured in the same position because the residual stress measurement method (energy-based method) used in this paper will generate a small hole in the measured position, which will disturb the original distribution of machining-induced residual stress. The theory to predict machining-induced residual stress is based on the theory of elastoplastic mechanics; therefore, the workpiece material is considered as a homogeneous and isotropic medium. Based on this hypothesis, for the same cutting parameter, the residual stresses on different positions of machined surface should be the same. However, the actual material is not a homogeneous and isotropic medium, which will cause the machining-induced residual stress on different positions of the machined surface to not be always the same. In this paper, in order to reduce the difference of machining-induced residual stress caused by the inhomogeneity of workpiece material, the experimental samples were selected in the adjacent area in the same casting material. Even though the inhomogeneity of the workpiece material is always existing, the difference among the data from the nine sample points cannot be avoided. To some extent, the average value of the nine sample points is used to "homogenize" the workpiece material. Except for measurement errors, the variance and standard deviation reflect the inhomogeneity of the workpiece material. Its research should be the task of the casting of material and belongs to the subject of material. The intention of this paper is to provide the knowledge of the adjustment of machining-induced residual stress based on the hypothesis of elastoplastic mechanics.

Using the experimental data in Table 2, fitting curves for each machining parameter and the residual stress could be obtained using the smoothing spline fitting method in Matlab, as shown in Fig. 3. Using the Matlab function "feval(fitmodel1,x)", the value of the fitting function for each input parameter "x" could be computed.

2.2 Linear inversion for adjustment of five-axis milling-induced residual stress

According to the theory presented by Huang and Yang [16] that was discussed in Section 1, the general equations for parameter inversion for residual stress adjustment are in the form of Eqs. (1)–(5). For the five-axis milling in this study, the six input parameters of cutting speed, front obliquity, side dip angle, feed rate, depth of cut, and residual height are represented by A_1, A_2, A_3, A_4, A_5, and A_6, respectively. Their reference values are represented by a_{10}, a_{20}, a_{30}, a_{40}, a_{50}, and a_{60}, respectively. The corresponding reference residual stress is represented by $H(a_{10}, a_{20}, a_{30}, a_{40}, a_{50}, a_{60})$. Changes in the residual stress caused by changes in the input parameters are represented by $\Delta O^{A_1}, \Delta O^{A_2}, \Delta O^{A_3}, \Delta O^{A_4}, \Delta O^{A_5}$, and ΔO^{A_6}, respectively. These changes in residual stress and their corresponding input parameters can be calculated using the smooth spline fitting curves presented in Section 2.1.

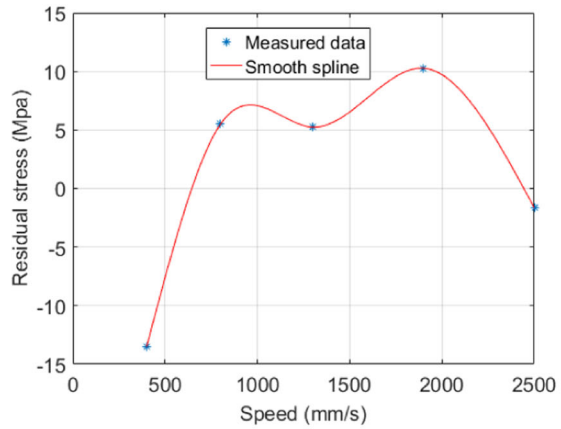

(a) Cutting speed vs. residual stress

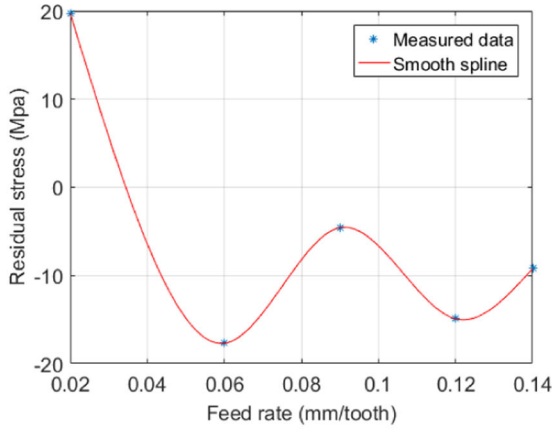

(b) Feed rate vs. residual stress

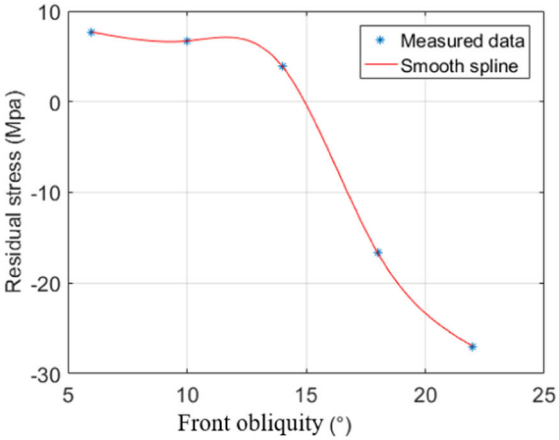

(c) Front obliquity vs. residual stress

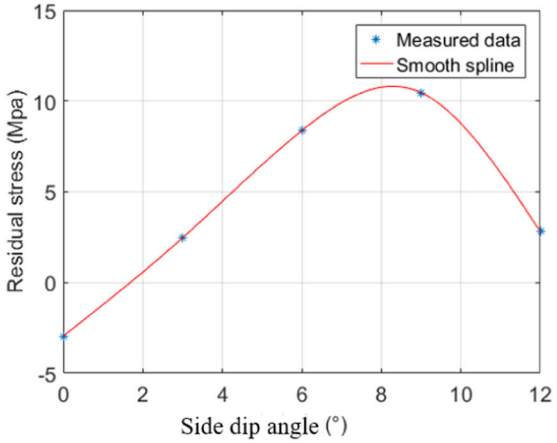

(d) Side dip angle vs. residual stress

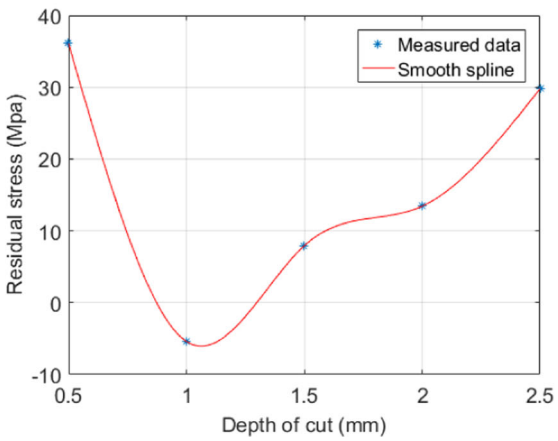

(e) Depth of cut vs. residual stress

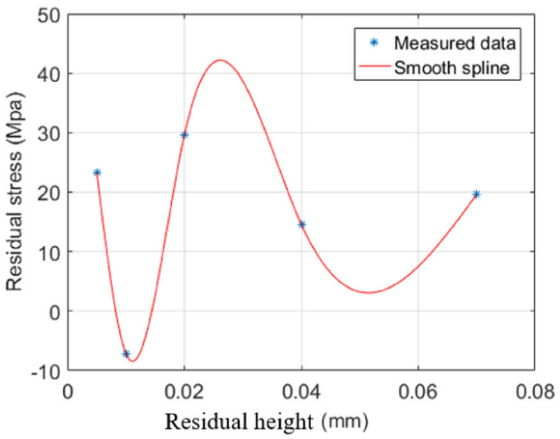

(f) Residual height vs. residual stress

Fig. 3 Smooth spline fitting curves for the input parameters with residual stress. **a** Cutting speed vs. residual stress, **b** feed rate vs. residual stress, **c** front obliquity vs. residual stress, **d** side dip angle vs. residual stress, **e** depth of cut vs. residual stress, **f** residual height vs. residual stress

The expected residual stress is represented by C_0. More details regarding parameter inversion can be found in [16]. Note that the equations for parameter inversion can also be used to calculate the residual stress when the input parameters are known. In this case, the parameter C_0 in Eq. (4) is an unknown parameter.

$$\Delta O = \sum_{i=1}^{n} \Delta O^{A_i} \tag{1}$$

Table 3 Input parameter levels

Symbol of input parameter	Input parameter	Level 1	Level 2	Level 3
A	Cutting speed	300 mm/s	650 mm/s	1500 mm/s
B	Feed rate	0.06 mm/tooth	0.09 mm/tooth	0.13 mm/tooth
C	Depth of cut	1 mm	1.6 mm	2.2 mm
D	Side dip angle	0°	4°	8°
E	Front obliquity	5°	10°	15°
F	Residual height	0.004 mm	0.02 mm	0.05 mm

$$\Delta O^{A_i} = O(A_i) - H(a_{10}, a_{20}, \ldots, a_{i0}, \ldots, a_{n0}) \quad (2)$$

$$\Delta O = O - H(a_{10}, a_{20}, \ldots, a_{i0}, \ldots, a_{n0}) \quad (3)$$

$$O = C_0 \quad (4)$$

$$\Delta O^{A_i} = C_i (i = 1, 2, \ldots, n-1) \quad (5)$$

3 Verification of residual stress adjustment for five-axis milling based on an orthogonal experiment with interaction of factors

In this section, to investigate the effectiveness of parameter inversion for reflecting the influence of machining parameters on residual stress, an orthogonal experiment with interactions of factors is conducted. This experiment can reveal the degree of influence of a machining parameter on the residual stress by the order of the residual stress range for each machining parameter. Thus, if the orders obtained with the experiment and parameter inversion are similar, it can be concluded that parameter inversion is effective to reflect the mechanism.

3.1 Design of the orthogonal experiment with interaction of factors

In the orthogonal experiment with interaction of factors, three input parameter levels are investigated, as listed in Table 3. Interactions between the cutting speed and feed rate ($A \times B$), cutting speed and depth of cut ($A \times C$), and front obliquity and feed rate ($B \times E$) are investigated. According to the principles for the design of orthogonal experiments with interaction of factors, an orthogonal table with $L_{27}(3^{13})$ is used. More details on using orthogonal experiments with interaction can be found in [18]. Correspondingly, the design of the orthogonal experiment with interactions of factors is summarized in Table 4.

3.2 Results of the orthogonal experiment

From the experimental design in Table 4 and input parameter levels in Table 3, the cutting conditions for the orthogonal experiment were determined, and are listed in Table 5. Machined workpieces produced using these cutting conditions are shown in Fig. 4. Residual stress measurements were again obtained based on the energy-based method. For each cutting condition, nine sample points were measured, and their average was used to represent the residual stress of the machining parameter (thus, the total number of sample points for all cutting conditions is $9 \times 27 = 243$). The original residual stress measurement data can be found in Table 9 of the Appendix.

In Table 5, the expected residual stresses were obtained using parameter inversion, as discussed in Section 2. Note that parameter inversion can also be used to calculate the residual stress from known input machining parameters. The residual stress range corresponding to each machining parameter reflects the degree of influence of that machining parameter on the residual stress. The descending order of the residual stress ranges of the machining parameters in Table 5 indicates that the order obtained with parameter inversion is very close to that in the experiment, with the exception of two parameters: residual height and depth of cut. Therefore, to some extent, parameter inversion is able to reflect the mechanism of

Table 4 Design of the orthogonal experiment with interaction of factors for five-axis milling

1	2	3	4	5	6	7	8	9	10	11	12	13
Cutting speed	Feed rate	Cutting speed × feed rate	Cutting speed × feed rate	Depth of cut	Cutting speed × depth of cut (front obliquity × feed rate)	Cutting speed × depth of cut	Side dip angle	Front obliquity	Residual height	Error	Front obliquity × feed rate	Error
A	*B*	*A* × *B*	*A* × *B*	*C*	*A* × *C* (*B* × *E*)	*A* × *C*	*D*	*E*	*F*		*B* × *E*	

Table 5 Experimental and expected residual stresses for the orthogonal experiment with interaction of factors and analysis of their range

No.	1 Cutting speed *A*	2 Feed rate *B*	3 Cutting speed × feed rate *A* × *B*	4 Cutting speed × feed rate *A* × *B*	5 Depth of cut *C*	6 Cutting speed × depth of cut (front obliquity × feed rate) *A* × *C* (*B* × *E*)	7 Cutting speed × depth of cut *A* × *C*	8 Side dip angle *D*	9 Front obliquity *E*	10 Residual height *F*	11 Error	12 Front obliquity × feed rate *B* × *E*	13 Error	Measured residual stress (MPa)	Expected residual stress (MPa)
1	1	1	1	1	1	1	1	1	1	1	1	1	1	8.88	− 30.44
2	1	1	1	1	2	2	2	2	2	2	2	2	2	10.29	− 10.58
3	1	1	1	1	3	3	3	3	3	3	3	3	3	− 0.59	− 29.56
4	1	2	2	2	1	1	1	2	2	2	3	3	3	− 28.45	− 13.03
5	1	2	2	2	2	2	2	3	3	3	1	1	1	− 22.08	− 24.57
6	1	2	2	2	3	3	3	1	1	1	2	2	2	− 5.22	6.32
7	1	3	3	3	1	1	1	3	3	3	2	2	2	− 5.96	− 49.09
8	1	3	3	3	2	2	2	1	1	1	3	3	3	− 11.48	− 10.76
9	1	3	3	3	3	3	3	2	2	2	1	1	1	− 9.36	1.66
10	2	1	2	3	1	2	3	1	2	3	1	2	3	10.95	− 40.26
11	2	1	2	3	2	3	1	2	3	1	2	3	1	− 12.73	3.72
12	2	1	2	3	3	1	2	3	1	2	3	1	2	− 4.58	24.97
13	2	2	3	1	1	2	3	2	3	1	3	1	2	23.39	1.26
14	2	2	3	1	2	3	1	3	1	2	1	2	3	− 12.80	29.97
15	2	2	3	1	3	1	2	1	2	3	2	3	1	− 6.18	− 3.50
16	2	3	1	2	1	2	3	3	1	2	2	3	1	3.86	5.44
17	2	3	1	2	2	3	1	1	2	3	3	1	2	10.23	− 20.58
18	2	3	1	2	3	1	2	2	3	1	1	2	3	49.44	15.95
19	3	1	3	2	1	3	2	1	3	2	1	3	2	9.02	− 14.59
20	3	1	3	2	2	1	3	2	1	3	2	1	3	− 18.42	− 9.50
21	3	1	3	2	3	2	1	3	2	1	3	2	1	1.84	31.39
22	3	2	1	3	1	3	2	2	1	3	3	2	1	7.09	− 11.96
23	3	2	1	3	2	1	3	3	2	1	1	3	2	26.01	36.38
24	3	2	1	3	3	2	1	1	3	2	2	1	3	− 6.35	22.17
25	3	3	2	1	1	3	2	3	2	1	2	1	3	− 19.20	11.86
26	3	3	2	1	2	1	3	1	3	2	3	2	1	5.04	5.09
27	3	3	2	1	3	2	1	2	1	3	1	3	2	37.22	2.73
Range analysis of the experimental results															
I(*j*)	**− 7.11**	**0.52**	**12.10**	**5.12**	**1.06**	**2.86**	**− 0.90**	**1.66**	**0.51**	**6.77**	**10.81**	**− 4.16**	**−**		
II(*j*)	6.84		− 4.34	0.02	− 2.88	5.29	1.37	6.50	− 0.43	− 3.70		6.74	2.-63 11.16		

Table 5 (continued)

No.	1 Cutting speed *A*	2 Feed rate *B*	3 Cutting speed × feed rate *A* × *B*	4 Cutting speed × feed rate *A* × *B*	5 Depth of cut *C*	6 Cutting speed × depth of cut (front obliquity × feed rate) *A* × *C* (*B* × *E*)	7 Cutting speed × depth of cut *A* × *C*	8 Side dip angle *D*	9 Front obliquity *E*	10 Residual height *F*	11 Error	12 Front obliquity × feed rate *B* × *E*	13 Error	Measured residual stress (MPa)	Expected residual stress (MPa)
III(*j*)	4.69	−2.73	− 3.33	− 0.71	6.25	− 3.73	3.96	− 3.17	4.35	1.36	−6.66	1.85	−4.10		
Max(*j*)	6.84	6.64	12.10	5.12	6.25	5.29	3.96	6.50	4.35	6.77	10.81	6.74	11.16		
Min(*j*)	− 7.11	−2.73	− 4.34	− 0.71	− 2.88	− 3.73	− 0.90	− 3.17	− 0.43	− 3.70	−6.66	− 4.16	−4.10		
Remarks: *I*(*j*), *II*(*j*), and *III*(*j*) represent the average residual stress for each input parameter level, respectively, in column *j*, and Max(*j*) and Min(*j*) represent the maximum and minimum value of *I*(*j*), *II*(*j*), and *III*(*j*), respectively (*j* = 1, 2, 3,…, 13)															
Range of each column	13.95	9.37	16.43	5.83	9.13	9.02	4.86	9.66	4.78	10.47	17.47	10.90	15.26		
Descending order of machining parameters according to their range:											Cutting speed (13.95) > *residual height (10.47)* > side dip angle (9.66) > feed rate (9.37) > *depth of cut (9.13)* > front obliquity (4.78)				
Range analysis of expected results															
I(*j*)	− 17.78	−8.32	− 2.57	− 2.57	−15.64	− 2.57	− 2.57	− 9.62	0.75	7.30	−2.57	− 2.57	−2.57		
II(*j*)	1.89	4.78	− 2.57	− 2.57	− 0.09	− 2.57	− 2.57	− 2.19	− 0.74	5.68	−2.57	− 2.57	−2.57		
III(*j*)	8.18	−4.19	− 2.57	− 2.57	8.01	− 2.57	− 2.57	6.82	− 7.73	− 20.70	−2.57	− 2.57	−2.57		
Max(*j*)	8.18	4.78	− 2.57	− 2.57	8.01	− 2.57	− 2.57	6.82	0.75	7.30	−2.57	− 2.57	−2.57		
Min(*j*)	− 17.78	−8.32	− 2.57	− 2.57	−15.64	− 2.57	− 2.57	− 9.62	− 7.73	− 20.70	−2.57	− 2.57	−2.57		
Range of each column	25.96	13.10	0.00	0.00	23.66	0.00	0.00	16.43	8.49	28.00	0.00	0.00	0.00		
Descending order of machining parameters according to their range:											*Residual height (28.00)* > cutting speed (25.96) > *depth of cut (23.66)* > side dip angle (16.43) > feed rate (13.1) > front obliquity (8.49)				

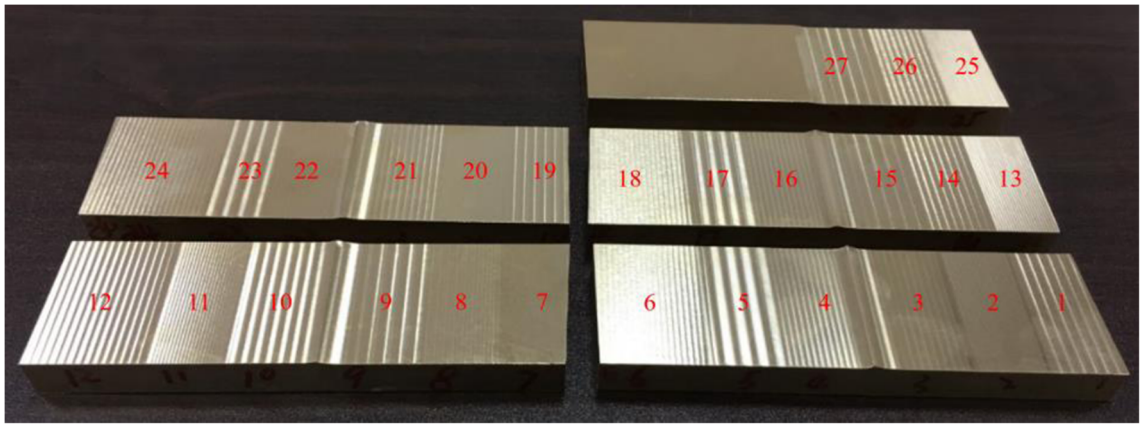

Fig. 4 Workpiece machined using the cutting conditions in Table 5

influence of the machining parameters on the residual stress. Also, based on the comparison, for further research, the theoretical model should be improved for more accurate results.

It is worth noting that the ranges obtained using parameter inversion for the interaction columns (including columns 3, 4, 6, 7, and 12) in Table 5 are equal to zero, which means that there is no interaction between these parameters based on the prediction of parameter inversion. This is because in the theory of residual stress adjustment based on parameter inversion, the fitting curve for a machining parameter with the residual stress is a

Table 6 Expected residual stress (C_0) and assignment of change in residual stress (C_i, i = 1, 2,…, 6)

	1 C_6 (for residual height ΔO^{A_6} (MPa))	2 C_4 (for feed rate ΔO^{A_4} (MPa))	3 C_1 (for cutting speed ΔO^{A_1} (MPa))	4 C_2 (for front obliquity ΔO^{A_2} (MPa))	5 C_3 (for side dip angle ΔO^{A_3} (MPa))	6 C_5 (for depth of cut ΔO^{A_5} (MPa))	7 C_0 (for expected residual stress O (MPa))
1	26.35	− 22.56	− 17.59	3.46	5.87	31.24	31.65
2	10.55	− 22.56	− 17.70	3.89	5.89	31.24	16.19
3	18.45	− 9.46	− 17.59	2.81	3.49	8.55	11.13
4	− 12.03	− 9.46	− 34.50	− 31.89	− 2.42	− 7.51	− 92.93
5	10.55	− 22.56	− 34.10	− 31.89	− 7.83	− 10.27	− 91.22
6	− 3.44	− 22.56	− 20.01	− 31.89	− 7.83	− 10.27	− 91.12
7	18.45	− 22.56	− 9.74	− 31.89	− 7.83	− 10.27	− 58.96
8	− 12.03	− 9.46	− 33.27	− 0.99	− 2.42	− 10.27	− 63.56
9	18.45	− 22.56	− 20.49	2.81	5.87	42.51	31.46
10	10.55	− 22.56	− 19.40	2.81	5.87	45.77	27.93
11	− 3.44	− 22.56	− 20.42	2.33	− 2.42	53.03	11.40
12	− 12.03	− 9.46	− 10.11	− 31.89	− 7.83	3.04	− 63.40
13	10.55	− 22.56	− 16.15	− 0.99	0.95	3.04	− 20.28
14	18.45	− 22.56	− 22.97	2.81	− 7.83	3.04	− 24.18
15	18.45	− 22.56	− 33.30	3.29	− 7.83	3.04	− 34.03
16	− 3.44	− 22.56	− 20.25	3.68	− 2.42	3.04	− 37.07
17	18.45	− 9.46	− 34.89	− 27.97	− 2.42	3.04	− 48.37
18	18.45	− 22.56	− 11.29	− 23.65	− 7.83	3.04	− 38.96
19	− 12.03	− 22.56	− 9.56	− 18.61	− 2.42	3.04	− 57.26
20	− 12.03	− 14.29	− 25.96	− 0.99	− 2.42	3.04	− 47.77
21	10.55	− 22.56	− 9.42	− 0.99	− 2.42	3.04	− 16.92
22	− 3.44	− 22.56	− 10.75	− 0.99	− 2.42	3.04	− 32.25
23	18.45	− 22.56	− 19.03	− 0.99	− 7.83	3.04	− 24.04
24	− 12.03	− 9.46	− 16.77	1.09	5.87	3.04	− 23.38
25	26.35	− 22.56	− 25.96	− 2.07	− 2.42	24.91	3.13
26	18.45	− 22.56	− 20.88	2.81	3.49	24.91	11.10
27	10.55	− 22.56	− 16.15	3.22	5.87	24.91	10.72
28	− 12.03	− 9.46	− 16.15	3.53	5.89	24.91	1.57
29	− 3.44	− 22.56	− 18.15	3.74	5.92	24.91	− 4.71
30	− 12.03	− 9.46	− 21.76	3.82	− 2.42	24.91	− 12.06

Table 7 Machining parameters calculated based on Table 6 with the corresponding measured and expected residual stresses

	1 Residual height (mm)	2 Feed rate (mm/tooth)	3 Cutting speed (mm/s)	4 Front obliquity (°)	5 Side dip angle (°)	6 Depth of cut (mm)	7 Measured results (MPa)	8 Expected residual stress (MPa)	9 Difference between expected results and measured results (MPa)	10 Product of measured and expected results (MPa^2)
1	0.004	0.06	413.3	4.6	8	0.5	− 3.35	31.65	35.01	− 106.10
2	0.006	0.06	411.5	3	8.5	0.5	− 61.23	16.19	77.42	− 991.25
3	0.005	0.09	413.3	6	6	2	9.16	11.13	1.96	101.97
4	0.01	0.09	93.8	22	3	1.231	− 9.96	− 92.93	− 82.97	925.44
5	0.006	0.06	104.2	22	0	1	− 16.95	− 91.22	− 74.26	1546.53
6	0.008	0.06	372.9	22	0	1	− 12.83	− 91.12	− 78.29	1169.50
7	0.005	0.06	548.8	22	0	1	− 67.36	− 58.96	8.40	3971.44
8	0.01	0.09	124.4	14	3	1	− 12.13	− 63.56	− 51.44	770.77
9	0.005	0.06	364.8	6	8	0.4	0.71	31.46	30.76	22.27
10	0.006	0.06	383.1	6	8	0.37	8.79	27.93	19.14	245.55
11	0.008	0.06	366.0	7	3	0.3	− 2.33	11.40	13.73	− 26.56
12	0.01	0.09	542.1	22	0	1.5	− 17.87	− 63.40	− 45.53	1132.63
13	0.006	0.06	437.5	14	4.67	1.5	− 48.13	− 20.28	27.85	975.79
14	0.005	0.06	322.9	6	0	1.5	− 44.26	− 24.18	20.08	1070.16
15	0.005	0.06	123.8	5	0	1.5	− 31.41	− 34.03	− 2.62	1068.80
16	0.008	0.06	369.0	4	3	1.5	− 31.68	− 37.07	− 5.39	1174.18
17	0.005	0.09	83.3	19.9	3	1.5	− 23.16	− 48.37	− 25.21	1120.24
18	0.005	0.06	520.8	18.5	0	1.5	− 17.71	− 38.96	− 21.25	689.88
19	0.01	0.06	552.1	17.41	3	1.5	− 13.64	− 57.26	− 43.62	780.91
20	0.01	0.043	270.8	14	3	1.5	− 27.64	− 47.77	− 20.13	1320.08
21	0.006	0.06	554.6	14	3	1.5	− 23.73	− 16.92	6.81	401.48
22	0.008	0.06	530.4	14	3	1.5	8.35	− 32.25	− 40.60	− 269.38
23	0.005	0.06	389.4	14	0	1.5	− 52.63	− 24.04	28.60	1265.10
24	0.01	0.09	427.1	13.16	8	1.5	− 33.62	− 23.38	10.24	786.08
25	0.004	0.06	270.8	14.3	3	2.5	− 39.32	3.13	42.45	− 123.17
26	0.005	0.06	358.3	6	6	2.5	− 17.13	11.10	28.23	− 190.14
27	0.006	0.06	437.5	5.16	8	2.5	− 32.34	10.72	43.06	− 346.79
28	0.01	0.09	437.5	4.44	8.5	2.5	− 57.74	1.57	59.31	− 90.74
29	0.008	0.06	404.0	3.8	8.2	2.5	− 43.10	− 4.71	38.39	202.91
30	0.01	0.09	343.5	2	3	2.5	− 23.80	− 12.06	11.74	286.91
Analysis of the experiment results										
Average of the difference between the measured results and expected results: 0.3951 (MPa)				Number of positive values for the product of the measured results and expected results: 22			Number of negative values for the product of the measured results and expected results: 8		Percentage of positive values in the product of the measured results and expected results: 22 ÷ 30 × 100% = 73.33%	

Fig. 5 Workpieces machined based on the cutting conditions in Table 7

single-variable function, and thus, the interaction of different machining parameters on the residual stress cannot be considered. Further research is necessary to reveal these interactions.

4 Verification of five-axis milling-induced residual stress adjustment based on randomly setting the expected residual stress

The verification based on the orthogonal experiment in the previous section focused on the significance of the influence of the machining parameters on the residual stress. In the orthogonal experiment, the combination of machining parameters is not random, which may not always meet the requirements of actual manufacturing. In industrial applications, the difference between the expected and measured residual stress, and the accuracy of the prediction of compressive and tensile residual stress are of concern. Thus, in this section, the expected residual stress is set randomly in order to verify the correctness of parameter inversion for five-axis milling-induced residual stress adjustment.

The expected residual stresses and assigned change in residual stress for each machining parameter are listed in Table 6. The corresponding machining parameters can then be computed using the theory of parameter inversion, as listed in Table 7. In order to decrease the influence of interactions between the machining parameters on the residual stress, the values of the machining parameters should be as close as possible to the reference values. Also, to reduce the roughness of the machined workpiece, the feed rate and residual height should be relatively small. Machined workpieces are shown in Fig. 5. The residual stress measurement was again based on the energy-based method. For each cutting condition in Table 7, nine sample points were measured, and their average was used to represent the residual stress of that machining parameter (thus, the total number of sample points for all cutting conditions is $9 \times 30 = 270$). Original residual stress measurement data can be found in Table 10 of the Appendix.

For the experimental and predicted results in Table 7, the average difference between the measured and expected results for the 30 cutting conditions is only 0.3951 MPa, which is very close to zero. This indicates that residual stress prediction using parameter inversion is effective statistically, even though the difference for each cutting condition is significant. Moreover, for the product of the measured and expected results, the percentage of positive numbers is 73.33%, which means that the correctness of the prediction for compressive and tensile residual stress is 73.33%. Without residual stress adjustment, this correctness will be only 50% because the induced residual stress caused by machining will be random, as with a coin toss that has a probability of 50%. Note that the expected residual stress is random, and nine sample points were measured for each cutting condition, and thus, to some extent, the analysis of the results of 30 total cutting conditions for this verification is reliable. The proposed residual stress adjustment based on parameter inversion is applicable for five-axis milling.

5 Conclusion

In this study, an experimental investigation of the application of parameter inversion for residual stress adjustment in five-axis milling was conducted using two methods: with an orthogonal experiment with interaction of factors and by randomly setting the expected residual stress. The following conclusions can be drawn from the study:

(1). The significance of the influence of the machining parameters on the residual stress obtained with parameter inversion is close to that obtained experimentally, which demonstrates that parameter inversion is able to reflect the mechanism of influence of the machining parameters on the residual stress.
(2). The average difference between the measured and expected results for the 30 cutting conditions is only 0.3951 MPa, which is very close to zero. This indicates that the residual stress prediction using parameter inversion is statistically effective.
(3). Using parameter inversion, the correctness of the prediction of compressive and tensile residual stress for five-axis milling is 73.33%, which is higher than the 50% that is achievable without any adjustment.

In summary, the experimental investigation in this study demonstrates that residual stress adjustment based on parameter inversion is applicable for five-axis milling, and shows the potential of this adjustment method in industrial applications. Further research is necessary to improve the correctness of the residual stress adjustment.

Acknowledgments This work is supported by the Major State Basic Research Development Program of China (973 Program, Grant No. 2014CB046704). Special thanks to the Advanced Manufacturing and Technology Experiment Center (in the School of Mechanical Science and Engineering, Huazhong University of Science and Technology) and the Analysis and Testing Center of Huazhong University of Science and Technology for their help.

Appendix

Table 8 Original residual stress measurement data for the cutting conditions in Table 2

			1(MPa)	2 (MPa)	3 (MPa)	4 (MPa)	5 (MPa)	6 (MPa)	7 (MPa)	8 (MPa)	9 (MPa)	Average residual stress (MPa)
Feed rate	0.14	1	− 31.31	19.27	8.98	− 50.73	35.48	− 2.09	− 65.57	2.85	0.04	− 9.23
	0.12	2	− 25.35	− 16.53	12.02	− 24.87	− 55.10	34.46	− 29.09	− 11.79	− 17.95	− 14.91
	0.09	3	− 33.39	0.81	31.76	− 50.15	4.79	14.65	− 19.12	19.01	− 9.61	− 4.58
	0.06	4	− 15.75	− 28.52	− 16.90	− 34.98	8.91	− 18.85	− 21.18	− 56.17	24.26	− 17.69
	0.02	5	75.94	38.54	50.26	− 14.36	− 29.10	45.42	− 27.29	− 0.90	39.15	19.74
Cutting speed	2500	6	− 10.32	− 12.96	− 11.34	− 4.09	− 18.29	− 2.39	− 6.17	42.12	8.53	− 1.66
	1900	7	− 6.69	8.80	62.17	22.97	− 15.94	28.11	− 23.96	− 5.06	22.03	10.27
	1300	8	6.98	− 34.41	21.32	− 22.52	6.47	6.58	28.27	19.22	15.27	5.24
	800	9	26.40	34.20	38.52	− 64.85	15.73	8.87	− 23.34	23.21	− 9.36	5.49
	400	10	− 42.49	− 45.63	− 32.81	− 8.95	− 12.26	45.39	− 2.50	− 7.27	− 15.04	− 13.51
Front obliquity	22	11	− 53.07	2.62	− 33.05	− 14.78	7.09	− 55.98	− 35.77	− 46.40	− 13.71	− 27.01
	18	12	− 22.90	− 21.87	− 31.63	6.31	− 34.82	− 9.86	− 3.44	− 6.78	− 24.95	− 16.66
	14	13	− 37.68	− 40.01	− 9.10	− 11.23	− 8.80	29.62	42.96	7.22	62.07	3.89
	10	14	15.61	− 6.74	36.41	− 16.37	6.68	10.36	35.39	3.87	− 25.09	6.68
	6	15	13.17	16.66	− 18.70	60.87	2.85	− 10.68	22.96	17.10	− 35.02	7.69
Side dip angle	12	16	− 11.37	− 12.64	− 33.68	− 3.64	16.42	13.57	41.32	5.13	10.08	2.80
	9	17	2.33	− 7.69	30.30	30.18	70.23	16.04	− 4.88	− 16.03	− 26.35	10.46
	6	18	− 9.39	9.28	5.93	8.80	30.58	7.46	− 12.86	− 1.29	36.80	8.37
	3	19	− 23.05	− 11.98	− 6.76	18.75	0.22	5.82	− 1.26	13.49	26.92	2.46
	0	20	− 1.68	5.76	6.13	− 8.79	− 24.53	14.95	7.51	− 3.64	− 22.28	− 2.95
Residual height	0.07	21	− 27.57	3.00	34.32	3.56	42.36	17.21	46.70	40.63	16.25	19.61
	0.04	22	− 21.21	23.25	4.82	− 0.75	− 11.51	42.96	61.98	32.67	− 0.94	14.58
	0.02	23	− 7.39	16.78	56.80	55.39	17.00	37.78	− 4.13	43.59	50.70	29.61
	0.01	24	− 25.04	− 21.60	21.65	− 26.73	− 26.83	31.39	− 27.81	− 14.55	25.16	− 7.15
	0.005	25	14.79	− 1.04	22.12	15.79	51.62	10.96	59.40	18.87	17.44	23.33
Depth of cut	2.5	26	9.73	43.95	− 13.95	− 16.54	− 0.96	118.45	− 21.57	51.87	97.11	29.79
	2	27	− 0.43	15.35	16.99	− 10.70	55.55	26.05	10.42	− 7.16	14.81	13.43
	1.5	28	− 10.99	− 41.05	− 31.62	24.27	5.20	31.08	18.20	− 3.70	79.87	7.92
	1	29	− 23.35	− 4.42	7.49	− 15.21	− 4.01	− 15.37	− 3.64	− 2.79	12.78	− 5.39
	0.5	30	100.87	18.69	124.48	18.23	26.73	16.80	− 16.39	0.14	35.54	36.12

Table 9 Original residual stress measurement data for the cutting conditions in Table 5

	1 (MPa)	2 (MPa)	3 (MPa)	4 (MPa)	5 (MPa)	6 (MPa)	7 (MPa)	8 (MPa)	9 (MPa)	Average residual stress (MPa)
1	− 42.50	− 9.92	− 28.99	39.34	3.66	51.09	49.12	15.65	2.49	8.88
2	20.74	28.11	− 8.88	7.51	17.78	26.28	22.97	26.16	− 48.06	10.29
3	− 13.96	− 67.13	− 22.86	− 28.16	− 4.81	− 40.11	32.62	71.12	68.02	− 0.59
4	− 66.63	− 20.56	17.87	− 36.88	− 31.09	− 54.12	− 16.35	− 5.65	− 42.60	− 28.45
5	− 3.33	− 42.96	7.96	7.51	− 3.94	− 29.64	− 44.25	− 39.71	− 50.33	− 22.08
6	− 24.54	− 17.05	− 5.07	− 39.93	2.82	− 40.51	6.03	90.79	− 19.49	− 5.22
7	− 33.02	− 40.19	− 4.60	− 5.34	40.27	− 6.22	− 23.94	23.06	− 3.70	− 5.96
8	− 36.87	− 20.67	− 42.41	− 19.74	− 4.97	7.22	21.57	2.74	− 10.20	− 11.48
9	72.52	26.96	− 15.97	− 30.68	3.87	− 107.97	− 45.98	41.07	− 28.09	− 9.36
10	− 16.75	0.79	52.32	53.65	46.16	− 24.77	3.70	− 16.17	− 0.35	10.95
11	− 37.27	− 8.91	− 8.68	− 21.93	− 32.19	26.48	− 0.82	− 19.31	− 11.89	− 12.73
12	− 12.57	− 0.01	− 23.00	25.67	− 3.61	− 33.13	− 12.62	− 25.05	43.11	− 4.58
13	48.62	− 13.94	10.36	16.45	36.93	15.19	63.44	19.30	14.16	23.39
14	− 34.11	− 20.24	12.62	− 48.86	21.21	− 27.73	36.25	− 22.86	− 31.50	− 12.80
15	− 2.68	24.78	− 43.25	− 29.63	− 6.59	− 22.93	24.27	− 13.36	13.75	− 6.18
16	− 16.82	3.11	23.57	36.06	4.75	− 23.74	− 1.44	− 14.21	23.43	3.86
17	− 28.52	35.55	39.37	58.85	26.75	54.40	3.47	− 33.61	− 64.14	10.23
18	73.72	152.81	118.86	7.96	− 66.79	36.21	76.52	28.57	17.07	49.44
19	− 5.05	49.36	36.40	− 2.22	31.06	− 43.57	− 2.40	23.50	− 5.91	9.02
20	− 5.89	− 15.71	0.59	− 30.60	− 22.15	− 45.21	− 15.40	0.78	− 32.20	− 18.42
21	28.78	− 0.83	− 2.11	4.22	39.65	− 25.66	− 9.57	− 2.44	− 15.51	1.84
22	21.30	10.37	− 16.06	− 17.60	12.08	44.65	− 2.73	− 1.38	13.15	7.09
23	− 6.78	− 1.57	− 20.76	− 9.12	31.43	53.24	27.28	111.82	48.57	26.01
24	− 25.54	− 6.90	− 6.74	− 42.90	− 44.16	2.81	57.72	60.76	− 52.19	− 6.35
25	− 28.79	− 24.21	− 9.49	− 31.06	25.37	− 42.26	− 50.59	44.46	− 56.24	− 19.20
26	− 7.46	86.15	23.99	− 2.56	4.22	55.76	− 72.70	1.60	− 43.62	5.04
27	− 1.06	− 5.18	19.14	20.59	91.11	77.38	69.45	22.27	41.26	37.22

Table 10 Original residual stress measurement data for the cutting conditions in Table 7

	1 (MPa)	2 (MPa)	3 (MPa)	4 (MPa)	5 (MPa)	6 (MPa)	7 (MPa)	8 (MPa)	9 (MPa)	Average residual stress (MPa)
1	− 14.56	− 48.79	39.23	− 7.10	− 5.61	− 17.00	54.19	− 22.54	− 7.99	− 3.35
2	− 64.43	− 69.80	− 66.75	− 42.88	− 52.25	− 78.81	− 37.86	− 67.77	− 70.52	− 61.23
3	18.34	− 45.47	33.19	− 6.38	58.85	− 22.76	54.49	− 1.21	− 6.59	9.16
4	− 7.76	− 1.41	− 28.14	− 31.76	− 26.46	41.83	− 38.38	− 7.25	9.70	− 9.96
5	− 5.06	18.26	− 39.77	− 6.08	29.25	− 37.52	8.62	− 67.95	− 52.34	− 16.95
6	− 23.03	− 6.32	9.13	− 14.91	9.40	− 30.29	− 19.19	− 15.64	− 24.65	− 12.83
7	− 90.55	− 109.17	− 66.51	− 33.98	− 20.31	− 100.54	− 77.01	− 57.86	− 50.31	− 67.36
8	39.85	− 42.28	6.28	− 37.31	− 14.24	− 19.99	− 20.46	− 31.19	10.21	− 12.13
9	− 2.10	− 5.47	5.80	37.85	− 17.48	− 0.41	− 0.32	− 12.17	0.67	0.71
10	38.05	22.56	− 4.48	24.92	− 45.97	18.46	34.92	60.56	− 69.91	8.79
11	6.70	-42.96	− 13.12	− 6.33	− 44.30	7.20	15.06	− 15.08	71.86	− 2.33
12	36.46	− 18.20	− 13.11	− 7.01	− 44.09	− 27.56	− 2.45	− 32.45	− 52.40	− 17.87
13	− 25.49	4.54	− 57.99	− 24.24	− 24.44	− 69.42	− 91.81	− 72.56	− 71.75	− 48.13
14	− 36.67	− 23.74	− 23.20	− 81.48	− 59.58	− 18.95	− 58.07	− 41.01	− 55.64	− 44.26
15	− 80.58	24.11	− 72.18	− 56.30	− 31.71	− 20.16	0.28	− 30.68	− 15.47	− 31.41
16	− 41.10	− 26.57	− 63.92	− 10.70	− 29.91	− 27.31	− 43.31	3.36	− 45.61	− 31.68
17	− 53.42	− 1.89	− 71.95	− 29.55	− 33.76	− 42.78	54.66	23.26	− 53.02	− 23.16
18	− 32.76	− 0.95	− 23.39	− 41.31	54.05	− 55.47	− 28.05	− 38.69	7.21	− 17.71
19	− 42.37	6.04	− 28.72	2.81	− 12.30	− 29.81	− 8.11	− 39.11	28.83	− 13.64
20	− 58.34	7.90	18.80	− 50.86	− 86.07	3.89	− 52.98	19.01	− 50.08	− 27.64
21	− 50.99	− 28.06	− 23.85	− 8.55	− 39.16	0.59	− 11.43	− 0.87	− 51.24	− 23.73
22	2.72	3.38	23.35	22.36	10.13	− 39.61	− 16.17	− 27.58	96.60	8.35
23	− 31.71	− 67.91	− 57.12	− 28.16	− 76.65	− 47.68	− 41.65	− 70.49	− 52.32	− 52.63
24	− 39.95	− 8.71	− 55.67	− 56.57	− 9.32	− 48.96	− 41.11	− 12.99	− 29.31	− 33.62
25	− 67.69	− 56.69	− 79.60	− 15.95	− 56.69	− 39.35	− 42.80	− 1.40	6.33	− 39.32
26	− 30.85	− 6.32	− 32.51	− 3.82	− 26.48	38.09	− 19.82	− 39.06	− 33.38	− 17.13
27	− 2.45	− 42.37	− 42.01	− 53.58	− 39.97	− 15.61	21.74	− 80.31	− 36.47	− 32.34
28	− 60.37	− 78.82	− 14.20	− 52.59	− 71.65	− 68.19	− 42.17	− 89.61	− 42.05	− 57.74
29	− 45.07	− 73.32	− 83.66	− 57.82	− 86.98	− 9.68	− 1.81	− 31.93	2.38	− 43.10
30	3.12	− 7.41	− 5.43	− 45.41	− 9.69	− 69.46	− 17.50	− 19.41	− 43.00	− 23.80

References

1. Ghosh S, Rana VPS, Kain V, Mittal V, Baveja SK (2011) Role of residual stresses induced by industrial fabrication on stress corrosion cracking susceptibility of austenitic stainless steel. Mater Des 32(7):3823–3831. https://doi.org/10.1016/j.matdes.2011.03.012
2. Lazoglu I, Ulutan D, Alaca BE, Engin S, Kaftanoglu B (2008) An enhanced analytical model for residual stress prediction in machining. CIRP Ann - Manuf Technol 57(1):81–84. https://doi.org/10.1016/j.cirp.2008.03.060
3. Ulutan D, Lazoglu I, Dinc C (2009) Three-dimensional temperature predictions in machining processes using finite difference method. J Mater Process Technol 209(2):1111–1121. https://doi.org/10.1016/j.jmatprotec.2008.03.020
4. M'Saoubi R, Chandrasekaran H (2011) Experimental study and modelling of tool temperature distribution in orthogonal cutting of AISI 316L and AISI 3115 steels. Int J Adv Manuf Technol 56(9-12):865–877. https://doi.org/10.1007/s00170-011-3257-y
5. Huang K, Yang W, Chen Q, He S (2016) An experimental investigation of temperature distribution in workpiece machined surface layer in turning. Int J Adv Manuf Technol 85(5):1207–1215. https://doi.org/10.1007/s00170-015-8016-z
6. Komanduri R, Hou ZB (2000) Thermal modeling of the metal cutting process: part I—temperature rise distribution due to shear plane heat source. Int J Mech Sci 42(9):1715–1752. https://doi.org/10.1016/S0020-7403(99)00070-3
7. Huang K, Yang W (2016) Analytical model of temperature field in workpiece machined surface layer in orthogonal cutting. J Mater Process Technol 229:375–389. https://doi.org/10.1016/j.jmatprotec.2015.07.008
8. Huang K, Yang W, Chen Q (2015) Analytical model of stress field in workpiece machined surface layer in orthogonal cutting. Int J Mech Sci 103:127–140. https://doi.org/10.1016/j.ijmecsci.2015.08.020
9. Huang K, Yang W (2016) Analytical modeling of residual stress formation in workpiece material due to cutting. Int J Mech Sci 114:21–34. https://doi.org/10.1016/j.ijmecsci.2016.04.018
10. Huang K, Yang W (2017) Analytical analysis of the mechanism of effects of machining parameter and tool parameter on residual stress based on multivariable decoupling method. Int J Mech Sci 128-129:659–679. https://doi.org/10.1016/j.ijmecsci.2017.05.031

11. Chen W, Vanboven G, Rogge R (2007) The role of residual stress in neutral pH stress corrosion cracking of pipeline steels – part II: crack dormancy. Acta Mater 55(1):43–53. https://doi.org/10.1016/j.actamat.2006.07.021
12. Withers PJ (2007) Residual stress and its role in failure. Rep Prog Phys 70(12):2211–2264. https://doi.org/10.1088/0034-4885/70/12/r04
13. Arrazola PJ, Özel T, Umbrello D, Davies M, Jawahir IS (2013) Recent advances in modelling of metal machining processes. CIRP Ann - Manuf Technol 62(2):695–718. https://doi.org/10.1016/j.cirp.2013.05.006
14. Brinksmeier E, Gläbe R, Klocke F, Lucca DA (2011) Process signatures – an alternative approach to predicting functional workpiece properties. Procedia Eng 19:44–52. https://doi.org/10.1016/j.proeng.2011.11.078
15. Brinksmeier E, Klocke F, Lucca DA, Sölter J, Meyer D (2014) Process signatures – a new approach to solve the inverse surface integrity problem in machining processes. Procedia CIRP 13:429–434. https://doi.org/10.1016/j.procir.2014.04.073
16. Huang K, Yang W, Ye X (2018) Adjustment of machining-induced residual stress based on parameter inversion. Int J Mech Sci 135:43–52. https://doi.org/10.1016/j.ijmecsci.2017.11.014
17. Jin H, Yang W, Yan L (2012) Development of an improved energy-based method for residual stress assessment. Philos Mag 92(4):480–499. https://doi.org/10.1080/14786435.2011.616867
18. He W, Xue W, Tang B (2017) Optimization test design method and data analysis. Chemical Industry Press, Beijing